Research Academy for Young Scientists

Modelling of Nonlinear Random Water Waves Using Linear and Nonlinear Wave Theories

Tingxuan Dai
daitingxuan05@gmail.com

under the direction of
Parvathy Kunchi Kannan
Royal Institute of Technology
Department of Fluid Mechanics

July 12, 2023

*

Abstract

Mathematical models for describing ocean waves play an important role in coastal engineering. Different wave models make different assumptions for approximation of surface elevation and velocity. To investigate the validity of Stokes' wave theory, linear random wave theory, Wheeler stretching, and 2nd order random wave theory, calculations for surface elevation and horizontal velocities were made using the four models. The calculated surface elevations were compared to measurement data and the horizontal velocity profiles were compared between models. This study provides support for previous findings of linear random wave theory overpredicting horizontal velocities and Wheeler stretching underpredicting horizontal velocities. This study also found that linear random wave theory predicts the surface elevation more accurately than 2nd order random wave theory, which contradicts results from previous studies. The relatively poor accuracy of 2nd order random wave theory may be explained by uncertainties in the calculation of cut-off frequency. The unexpectedly high accuracy of linear random wave theory may be explained by the limitations of measurement data but this needs to be investigated further by comparing different spectral analysis techniques. This paper provides framework for further studies of wave models in different wave conditions with the aim of applying them in coastal engineering.

Acknowledgements

I would like to thank my mentor Parvathy Kunchi Kannan for giving me the opportunity to conduct this study. I am grateful for her invaluable help, encouragement and guidance throughout this project. I also want to thank Parvathy's supervisors Outi Tammisola and Shervin Bagheri. I want to express gratitude to my project partner Algot Kullberg for his support and excellent contribution of ideas. Special thanks to all of the organizers of Rays for making these weeks the most intense yet memorable four weeks of my life. I also want to thank Rays alumni for taking their time to give me valuable and detailed feedback. Finally, I could not have done this without Rays — for Excellence and their collaboration partners, AstraZeneca and Stiftelsen Lars Hiertas Minne.

Contents

Glossary

Figure 1 is illustration of a water wave. Symbols are defined in Table 1 and Table 2.

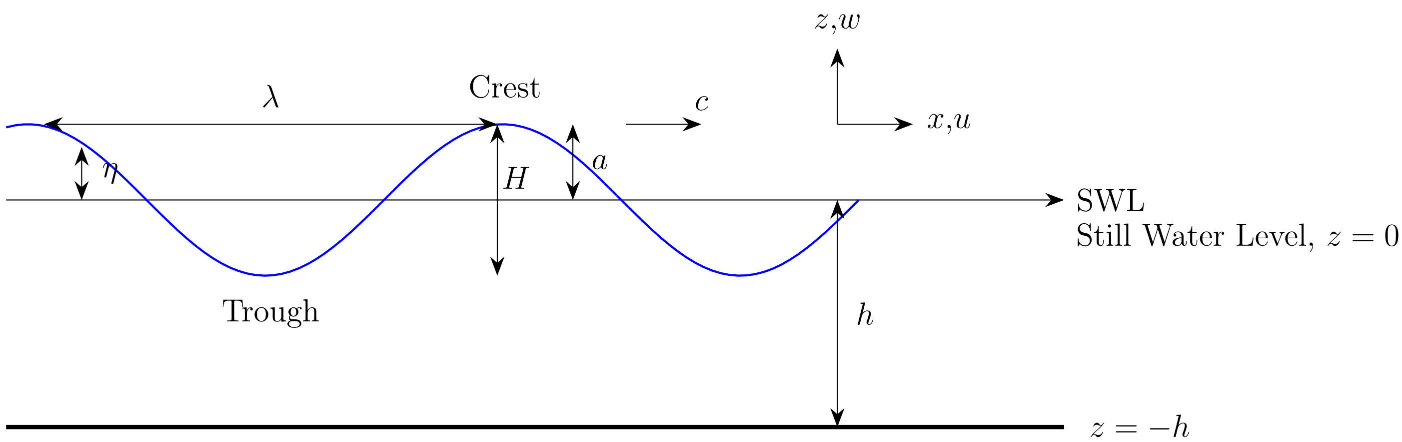

Figure 1: An illustration of a water wave.

Table 1: Definitions of symbols.

Symbol	Definition	Unit
H	wave height	m
η	water surface elevation from SWL	m
h	water depth	m
λ	wavelength	m
T	wave period	s
u	horizontal particle velocity	m/s
w	vertical particle velocity	m/s

Table 2: Definitions of calculated symbols.

Name	Definition
wave number	$k = \frac{2\pi}{\lambda}$
angular frequency	$\omega = \frac{2\pi}{T}$
wave amplitude	$a = \frac{H}{2}$
wave steepness	$s = \frac{H}{\lambda}$
phase velocity	$c = \frac{\lambda}{T}$

1 Introduction

Coastal engineering requires mathematical models that describe ocean waves. One issue to account for in construction of coastal structures is fatigue failure [1]. This mechanism refers to formation and growth of cracks on a material as a result of cyclic loads from ocean waves [1]. By modelling waves nearby a construction for an extended period of time, the long-term distribution of wave-induced loads can be analyzed, thus allowing fatigue assessment [2].

The main challenge in wave modelling is the nonlinear and irregular behavior of ocean waves. Ocean waves vary in height, direction and form as they propagate. Wave theories provide approximations for waves and model them as two-dimensional waves [3]. In this study, the validity and limitations of four different wave theories are investigated. First, a literature review is conducted to understand fundamental ocean wave concepts. Second, mathematical models are used to calculate surface elevation and horizontal velocities based on measurement data [4].

1.1 Regular Water Waves

Regular waves are periodic, they have a constant form that is repeated for each period in time and space. Regular waves can be described using linear regular wave theory, also known as Airy wave theory [3].

1.1.1 Assumptions for Linear Wave Theory

(A) Mass continuity applies, meaning that

$$\frac{\partial u}{\partial x} + \frac{\partial w}{\partial z} = 0 \tag{1}$$

where u is the velocity component in the direction of wave propagation and w is the velocity component in the direction perpendicular to the wave propagation [3].

(B) The motion is irrotational, which means that viscous forces and external forces are negligible, therefore

$$\frac{\partial w}{\partial x} - \frac{\partial u}{\partial z} = 0 \quad [3]. \tag{2}$$

Since the flow is irrotational, energy is conserved.

(C) The unsteady Bernoulli equation applies,

$$\rho \frac{\partial \phi}{\partial t} + p + \rho g z + \rho \left[\frac{\partial_x \phi^2 + \partial_y \phi^2}{2} \right] = \mathrm{C} \tag{3}$$

where ϕ is velocity potential, p is total pressure, g is gravitational acceleration $g = 9.81\,\mathrm{m/s^2}$, ρ is fluid density and C is a constant. Equation (3) states the relationship between fluid velocity, pressure and the potential energy, which ensures the conservation of energy followed from Equation (2). [3]

(D) The wave motion is periodic in horizontal position x and time t, meaning that the wave height η varies in a regular pattern [3].

(E) The wave amplitude a is small compared to the wavelength λ, ($a \ll \lambda$), since increased wave steepness s reduces the validity of Airy wave theory [3].

(F) The wave amplitude is small compared to water depth h, ($a \ll h$), which means that influence from the water bed on the wave is negligible [3].

1.1.2 Boundary Conditions for Linear Waves

Fluid particles near the surface are assumed to remain on the surface, as governed by the following kinematic free surface boundary condition.

$$w = \frac{\partial \eta}{\partial t} + \frac{\partial \eta}{\partial x} u \tag{4}$$

which can be linearised to Equation (5)

$$w \approx \frac{\partial \eta}{\partial t} \tag{5}$$

by evaluating at $z = 0$ instead of $z = \eta$. Based on the assumptions and boundary conditions for linear wave theory, the surface elevation η is given by the following equation.

$$\eta = a\sin(\omega t - kx) \tag{6}$$

where ω is the wave frequency and k is the wave number. [3]

The dynamic free surface boundary condition equates the pressure along the surface to the atmospheric pressure using Bernoulli equation,

$$g\eta + \frac{1}{2}\left(\left(\frac{\partial\phi}{\partial x}\right)^2 + \left(\frac{\partial\phi}{\partial z}\right)^2\right) + \frac{\partial\phi}{\partial t} = 0 \tag{7}$$

for $z = \eta$ [3]. The small amplitude assumption of linear regular wave theory allows the pressure for a linear wave to be evaluated at SWL where $z = 0$ and the nonlinear terms can be neglected to yield the linearised dynamic free surface boundary condition,

$$g\eta + \frac{\partial\phi}{\partial t} = 0 \quad [5]. \tag{8}$$

1.1.3 Phase Velocity for Linear Waves

Phase velocity is the speed of individual waves. The dispersion relationship, Equation (9), is used to find phase velocity.

$$\omega^2 = gk\tanh(kh) \tag{9}$$

Water waves are dispersive because waves of different wavelengths propagate with different phase velocities. Following Equation (9), the phase velocity c is given by,

$$c = \frac{\lambda}{T} = \frac{\omega}{k} = \left(\frac{g}{k}\tanh(kh)\right)^{\frac{1}{2}} \tag{10}$$

where T is the wave period. In deep water, i.e. $h > 0.5\lambda$, the approximation $\tanh(kh) = 1$ is made and dispersion relationship and phase velocity for deep water are,

$$\omega^2 = gk \quad \text{and} \quad c_o = \sqrt{\frac{g}{k}} \quad . \tag{11}$$

In shallow water, i.e. $h < 0.05\lambda$, the approximation $\tanh(kh) = kh$ is made and dispersion relationship and phase velocity for shallow water are,

$$\omega^2 = ghk^2 \quad \text{and} \quad c = \sqrt{gh}. \quad [6] \tag{12}$$

1.1.4 Stokes' Wave Theory

Stokes' wave theory is a nonlinear wave theory that is applied for waves with large wave steepness s [3]. Figure 2 shows a Stokes' wave. The wave is regarded as a sum or superposition of component waves called harmonics [7].

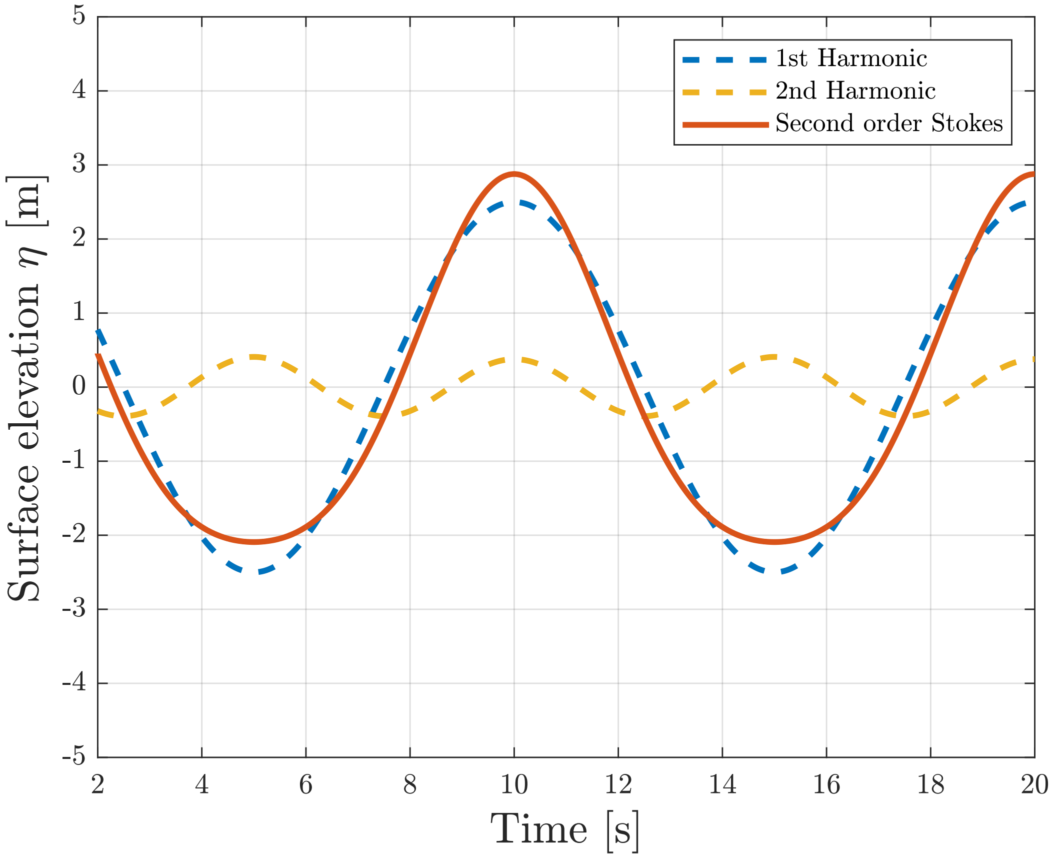

Figure 2: An illustration of a Stokes' 2$^{\text{nd}}$ order wave profile. The first harmonic (blue dashed line) and second harmonic (yellow dashed line) are plotted against the resulting 2$^{\text{nd}}$ order wave (red line).

The first harmonic is a linear component regarded as a free wave which satisfies the assumptions of linear wave theory. The higher order harmonics are bound waves. Bound waves are generated by interactions between waves and do not satisfy the dispersion relationship from Equation (9). In Figure 2, it can be observed that the 2nd order wave has taller crests and broader, flatter troughs compared to the first harmonic. Surface elevation for Stokes' 2nd order solution can be calculated using Equation (13).

$$\eta = \frac{H}{2}\cos(kx - \omega t) + \frac{H^2 k}{16}\frac{\cosh(kh)}{\sinh^3(kh)}(2 + \cosh(2kh))\cos[2(kx - \omega t)] \tag{13}$$

where the first term is the first harmonic and the second term is the second harmonic. The horizontal velocity is given by the following equation.

$$u = \frac{H}{2}\frac{gk}{\omega}\frac{\cosh[k(h+z)]}{\cosh(kh)}\cos(kx - \omega t) + \frac{3}{16}H^2\omega k\frac{\cosh[2k(h+z)]}{\sinh^4(kh)}\cos[2(kx - \omega t)]. \quad [3] \tag{14}$$

For Stokes' expansions of higher order, additional nonlinear terms are added for more accurate approximation. The appropriate order of Stokes' expansion is dependent on water depth and wave steepness. Stokes' wave theory is applicable for deep water conditions. The steeper the wave, the higher order of Stokes' expansion is required for accurate approximation. $\frac{H}{gT^2}$ is a relative measure for wave steepness. With calculated $\frac{H}{gT^2}$ and water depth h, the applicable Stokes' order is determined using a diagram developed by Le Méhauté. [8]

1.2 Random Waves

Ocean waves are in reality unsteady and not periodic, they are constructed of a number of waves interacting with each other [3].

1.2.1 Linear Random Wave Theory

A random wave system can be described by Linear Random Wave Theory, LRWT, as a superposition of a large number of regular linear waves of different amplitudes at random phase angles α_m travelling in the same direction. The surface elevation of linear random waves is given by Equation (15).

$$\eta = \sum_{m=1}^{M} a_m \cos(k_m x - \omega_m t + \alpha_m) \tag{15}$$

where a_m, k_m, ω_m and α_m are the amplitude, wave number, angular frequency and phase angle corresponding to the m^{th} wave and M is the total number of waves. The velocity is given by Equation (16).

$$u = \sum_{m=1}^{M} a_m \omega_m \frac{\cosh k_m(z+h)}{\sinh(k_m h)} \cos(k_m x - \omega_m t + \alpha_m). \quad [9] \tag{16}$$

Dispersion relationship from Equation (9) is applied to all of the waves in the system as LRWT assumes all waves being free waves. However, waves of different frequencies interact with each other and generate bound waves. The generated bound waves do not satisfy dispersion relationship. Steep waves contain bound waves that have smaller wave numbers k than their corresponding free waves. In LRWT, the larger wave numbers contribute to overestimated horizontal velocities. The impact from interactions between waves increase when approaching wave surface where $z = \eta$. Since LRWT evaluates boundary conditions at $z = 0$, overpredictions of horizontal velocities are made, this is referred to as high-frequency contamination. [10]

1.2.2 Wheeler Stretching

Wheeler Stretching is an empirically corrected wave theory based on LRWT. Wheeler stretching introduces an effective z-coordinate z^* as a function of water depth h and surface elevation η that can be calculated using Equation (17).

$$z^* = \frac{h(z-\eta)}{(h+\eta)} \tag{17}$$

Equation (17) sets $z^* = 0$ to the original surface elevation $z = \eta$. Applying Wheeler stretching, the horizontal velocity is given by,

$$u = \sum_{m=1}^{M} a_m \omega_m \frac{\cosh k_m(z^*+h)}{\sinh(k_m h)} \cos(k_m x - \omega_m t + \alpha_m). \quad [11] \tag{18}$$

Wheeler stretching introduces a new z-coordinate system and calculates the horizontal velocity using LRWT. z^* is lower than z, therefore Wheeler stretching yields smaller velocities than LRWT [12]. However, Wheeler stretching does not satisfy mass continuity [13].

1.2.3 2$^{\text{nd}}$ Order Random Wave Theory

The 2$^{\text{nd}}$ order random wave includes bound waves generated by interactions between two waves. The surface elevation approximated using Stokes' 2$^{\text{nd}}$ order wave theory have higher and narrower crests as well as broader and less deep troughs compared to the surface elevation approximated using LRWT [14]. These nonlinear effects are comparable to the observations seen in Figure 2 for Stokes' 2$^{\text{nd}}$ order expansion. A model of interactions between two random waves developed by Longuet-Higgins & Stewart can be found in Appendix A. Based on the two-wave interactions, a 2$^{\text{nd}}$ order random wave theory was proposed by Sharma & Dean and the equations are found in Appendix B.

In order to apply higher order random wave theories, bound waves have to be distinguished from free waves. If 2$^{\text{nd}}$ order random wave theory is applied to bound waves and free waves, unnecessary bound waves are generated from interactions between bound waves [15]. Since bound waves have higher frequencies than the spectral peak frequency of an amplitude spectrum [15], a low-pass filter is applied to eliminate bound waves. Based on experimental data, DNVGL-RP-C205 guidelines have proposed following equation for calculating cut-off angular frequency.

$$\omega_{max} = \sqrt{\frac{2g}{H_s}} \tag{19}$$

where H_s is the significant wave given by $H_s = 4\sigma$ where σ is the standard deviation of the wave heights and H_s denotes the average height of the 1/3 highest waves [16].

1.3 Previous Studies

Standberg have conducted numerical simulations for prediction of horizontal velocities u to evaluate the validity of 2$^{\text{nd}}$ order random wave model, LRWT, Wheeler's method and Grue's method. Grue's method is based on Stokes' 3$^{\text{rd}}$ order wave theory and is applied to individual waves without considering interactions between waves. The data used were measured elevation records from an experiment studying extreme events in a wave basin. It was found that 2nd order random wave theory gives the overall best fit for horizontal velocities. LRWT was found to notably overpredict velocities whereas Wheeler Stretching underpredicts the velocities. [12]

Similar patterns are attained by Spell et al. in a study comparing LRWT and a hybrid wave model using experimental data from a water basin [17]. The hybrid wave model is a 2nd order random wave theory with improved methods of distinguishing bound waves from free waves [18]. Results from these studies also show that the difference of LRWT drastically increases when approaching SWL [12, 17].

Multiple previous studies have shown that 2nd order wave theory predicts higher crests and flatter troughs in comparison to the surface elevation approximations made with LRWT. These studies have also concluded that 2nd order wave theory yields more accurate approximations for surface elevation than LRWT. [17, 19, 20]

1.4 Aim of the Study

Ocean waves are complex phenomena that can be described by mathematical modelling. There are water wave models that describe linear, nonlinear, random and regular waves. Linear wave theory is based on a number of assumptions that are seldom satisfied by real ocean waves. Coastal engineering requires accurate approximations of the ocean wave properties which have to account for interactions between waves. The aim of this study is to investigate the validity of four established water wave theories, Stokes' wave theory, LRWT, LRWT with Wheeler stretching and 2nd order random wave theory for approximating the surface elevation and horizontal velocities of nonlinear random waves.

2 Method

In this study, four different mathematical models were used to calculate surface elevation and horizontal velocities of nonlinear random waves. The used measurement data [4] had a significant wave height H_s of $H_s = 16.7\,\mathrm{m}$. Through spectral analysis, the wave surface elevation, see Appendix C, was decomposed into 50 component waves defined by wave frequency f, wave height, wave amplitude and phase angle. Measured velocities are not included in the measurement data and the technique for spectral analysis is not given.

Approximations for surface elevation η and horizontal velocity u were calculated using Stokes' wave theory, LRWT, LRWT with Wheeler stretching and 2^{nd} order random wave theory. By comparing the calculated data between models and with measurement data, the validity of the studied wave theories was compared.

2.1 Assumptions and Cut-off Frequency for 2^{nd} Order Random Wave Theory

The calculations are simplified by assuming the wave travelling in deep water. By letting water depth approach infinity, equations for 2^{nd} order random wave theory from Appendix B were simplified to the equations found in "Alternative methods of realizing the sea spectrum for time-domain simulations of marine structures in irregular seas" [21]. The cut-off angular frequency $\omega_{\max}$ was calculated to $\omega_{\max} = 0.87\,\mathrm{rad/s}$ using Equation (19) which was converted to linear frequency $f_{\max} = 0.17\,\mathrm{Hz}$. The studied amplitude spectrum can be found in Appendix D and only the frequencies lower than the cut-off frequency were included in the calculations.

2.2 Assumptions for Stokes' Wave Theory and Stokes' Order

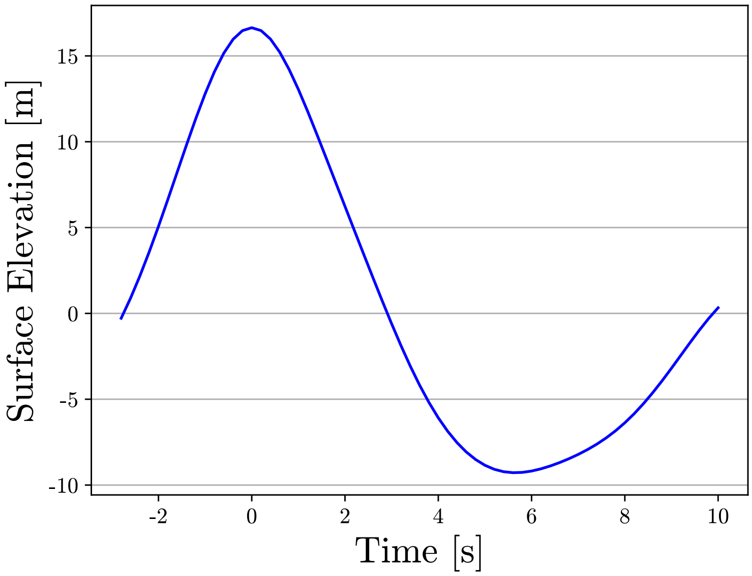

Figure 3: Measured water surface elevation for the studied wave in the time frame $-2.80\,\mathrm{s} \leq t \leq 10.0\,\mathrm{s}$ [4].

Stokes' wave theory was applied for the greatest wave height, H_{max}. Using zero-down crossing by finding the maximum difference between two consecutive maximum and minimum values of surface elevation η, the greatest wave height was found to be $H_{\mathrm{max}} = 25.9\,\mathrm{m}$. The corresponding wave period was $T = 12.4\,\mathrm{s}$. In order to compare different wave theories, the studied time frame shown in Figure 3 was set to $-2.80\,\mathrm{s} \leq t \leq 10.0\,\mathrm{s}$ where the highest wave was located. The order of Stokes' wave theory was chosen to be the 5^{th} order since the wave propagates in deep water and the measure for steepness $\frac{H}{gT^2} = 0.017$ corresponds to Stokes' 5^{th} order expansion. Equations for surface elevation and horizontal velocity using Stokes' 5^{th} order expansion are found in Appendix E.

2.3 Assumptions for LRWT and Wheeler Stretching

For LRWT and Wheeler stretching, the wave was assumed to only vary with time. The term kx_m was thus not included in Equation (15), Equation (16), and Equation (18).

3 Results

The results attained in this study are surface elevation and horizontal velocities calculated using each of the studied wave theories. The calculated values and plots with measurement data are presented in the following sections.

3.1 Horizontal Velocities

In Figure 4, the horizontal velocities, u, calculated with Stokes' theory, LRWT, Wheeler stretching and 2$^{\text{nd}}$ order wave theory are displayed with SWL at $z = 0$. Table 3 shows the maximum velocities calculated at the highest surface elevation where $z = 16.6\,\text{m}$.

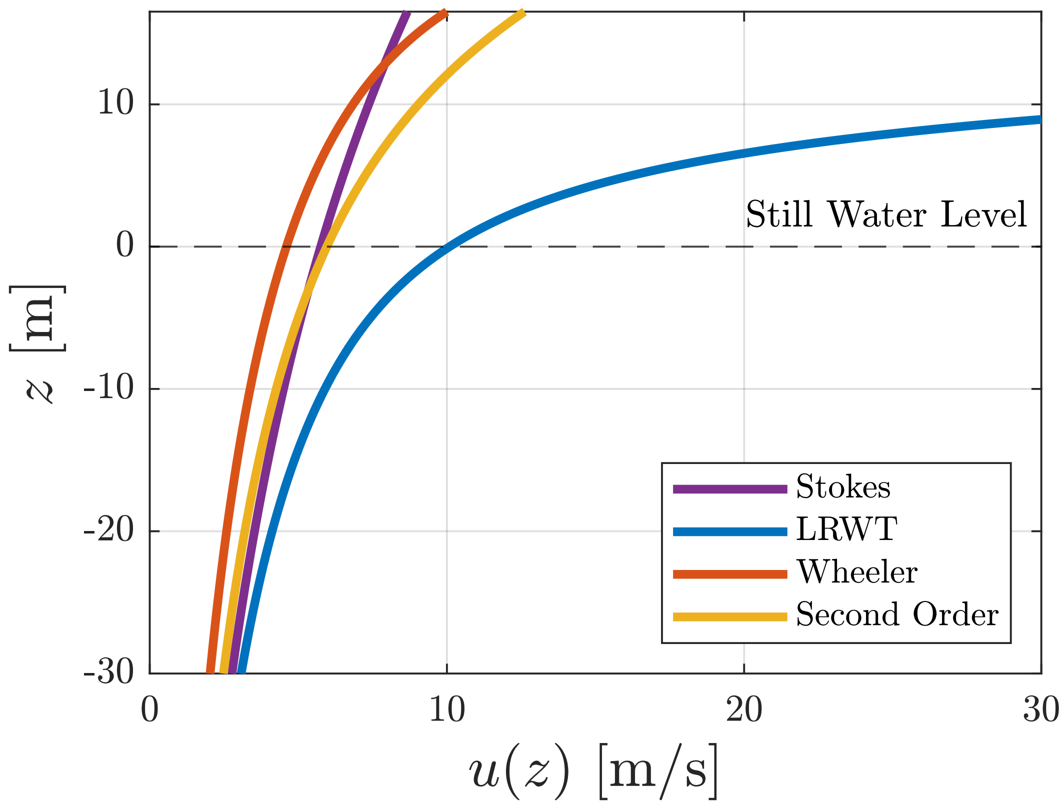

Figure 4: Velocity profiles for Stokes' wave theory, LRWT, Wheeler stretching and 2$^{\text{nd}}$ order random wave theory. SWL is the still water level where $z = 0$.

Table 3: Horizontal velocity calculated with each of the studied models at the highest surface elevation $z = 16.6\,\text{m}$.

Model	Velocity [m/s]
Stokes' wave theory	8.69
LRWT	5.48×10^5
Wheeler's stretching	10.4
2^{nd} order random wave theory	12.7

3.2 Surface Elevation

In Figure 5, the surface elevation η calculated using Stokes' theory, LRWT and 2^{nd} order wave theory are plotted against the measured surface elevation. Table 4 shows the R^2 values for calculated surface elevation fitted to measured data points.

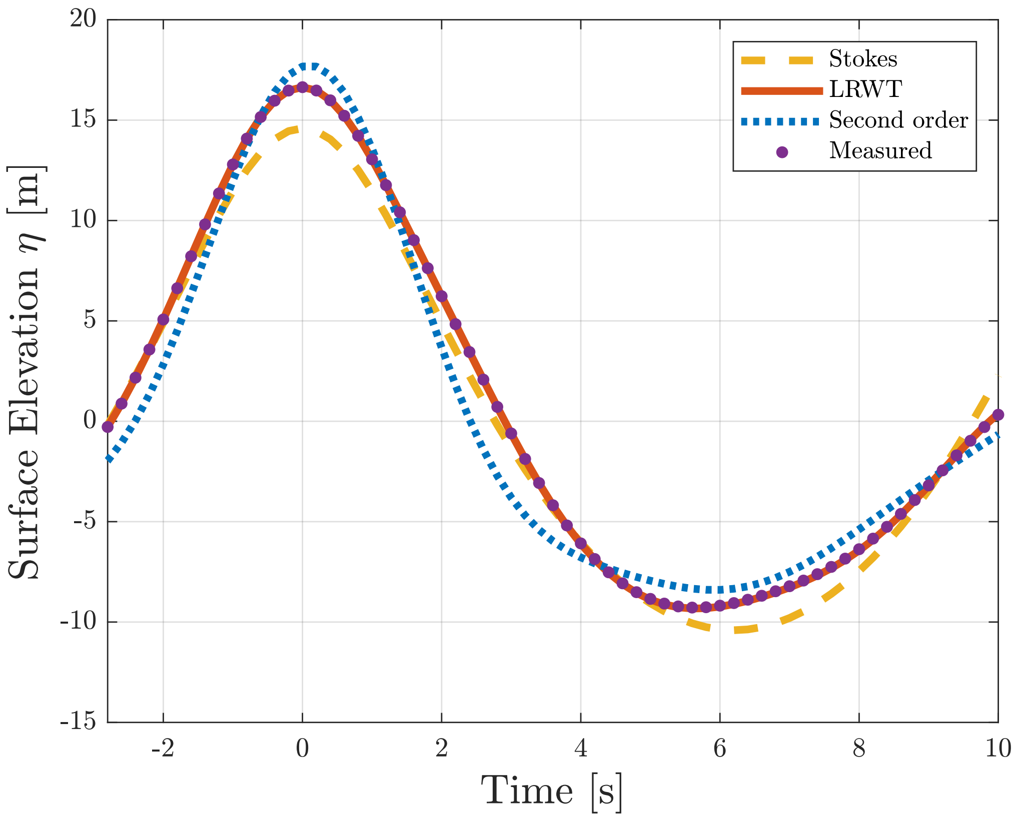

Figure 5: Approximated surface elevation using Stokes' wave theory (yellow dashed line), LRWT (red line) and 2^{nd} order random wave theory (blue dotted line) plotted against measured data points (purple dots).

Table 4: Coefficient of determination, R^2, for the surface elevations calculated with each of the studied models fitted to measured surface elevation.

Model	R^2
Stokes' wave theory	0.98
LRWT	1.00
2$^{\text{nd}}$ order random wave theory	0.97

4 Discussion

In this study, horizontal velocities are compared between the four wave models and LRWT is found to overpredict the horizontal velocities. Approximations for surface elevation using different models are compared to the measured surface elevation and the most accurate approximation is found to be given by LRWT. The spectral analysis of the measurement data and the cut-off frequency were two aspects that was found to be interesting.

4.1 Horizontal Velocities

In Figure 4, it can be observed that the horizontal velocities u calculated with LRWT are notably larger than the horizontal velocities calculated using the other wave theories, especially near SWL. Table 3 shows that LRWT gives an unrealistically large value of 548 000 m/s for maximum horizontal velocity. These results indicate that LRWT overpredicts horizontal velocities near SWL. The reason for overprediction is high-frequency contamination as a result of LRWT neglecting influences from bound waves [10]. As the wave approaches SWL, effects from bound waves increase and LRWT differs from the other theories [10]. Similar results where found in previous studies [12, 17].

Figure 4 shows that Wheeler stretching approximates lower velocities than LRWT and that 2$^{\text{nd}}$ order random wave theory gives values between Wheeler stretching and LRWT. This is in accordance with results from previous studies [12, 17]. In this study, measured velocities are not given, therefore an evaluation of the validity of different wave theories for velocity calculation cannot be made. However, the results indicate that Wheeler stretching underpredicts the horizontal velocities and that LRWT overpredicts them.

4.2 Surface Elevation

In Figure 5, it can be seen that the surface elevation profile approximated with 2nd order random wave theory has higher, narrower crests and broader, shallower troughs in comparison to the surface elevation calculated with LRWT. The difference in shape is caused by bound waves generated by interactions between waves [15] and confirms results from previous studies [17, 19, 20].

It can also be observed in Table 4 that the surface elevation calculated with LRWT has a perfect correlation, $R^2 = 1.000$, to the measured surface elevation in the studied time frame. This observation differs from results attained in previous studies [17, 19, 20] where 2nd order random wave theory was found to give the most accurate approximation.

LRWT regards all waves as free waves and reconstructs the original surface elevation by a summation of the decomposed waves. The technique for spectral analysis is not given in this study. However, the unexpected high accuracy of LRWT indicates that the technique for spectral analysis could have influenced the approximation. Depending on how the spectral analysis was conducted, the accuracy of LRWT for surface elevation approximation varies.

In this study, the calculation of cut-off frequency could have affected the accuracy of 2nd order random wave theory. Since a general guideline was followed, bound waves could have been included in the studied frequency range and contributed to deviations from the original measured surface elevation [15]. In addition, 2nd order random wave theory does not include the bound waves resulting from multi-wave interactions. A higher order wave theory is required for higher accuracy when large numbers of waves are involved.

Stokes' wave theory estimates the surface elevation for an individual wave that is assumed to repeat periodically. Therefore, Stokes' wave theory cannot represent an irregular wave system but it is applicable for characterizing a specific wave.

In this study, measurement data is limited. Measured velocities and information about the spectral analysis technique would enable deeper analysis of the validity of the tested models.

4.3 Further Studies

In order to further study the validity of 2^{nd} order random wave theory, different methods for determining cut-off frequency should be compared. To investigate the influence on LRWT from spectral analysis, different spectral analysis techniques should be implemented and compared. Applying the wave models on wave data from different wave conditions, such as different water depths, would allow applications in different coastal areas.

4.4 Conclusion

By comparing the calculated surface elevations, calculated horizontal velocities and measurement data, conclusions about the validity of different wave theories for approximating surface elevation and horizontal velocities have been drawn. It is concluded that LRWT gives the closest approximation for surface elevation of the studied wave despite previous studies finding 2^{nd} order random wave theory being more accurate. This can be explained by the spectral analysis conducted with the measured data and the choice of cut-off frequency for 2^{nd} order random wave theory. Furthermore, this study provides some support for Wheeler stretching underpredicting and LRWT overpredicting horizontal velocities. However, further studies are required for drawing more extensive conclusions about the validity of each wave model and the assumptions that have to be satisfied for implementing each model in coastal engineering.

References

[1] K. Karlén, *Probabilistic modeling of fatigue failures.* PhD thesis, KTH Royal Institute of Technology, 2012.

[2] L. De Gracia, H. Wang, W. Mao, N. Osawa, I. Rychlik, and G. Storhaug, "Comparison of two statistical wave models for fatigue and fracture analysis of ship structures," *Ocean Engineering*, vol. 187, p. 106161, 2019.

[3] R. G. Dean and R. A. Dalrymple, *Water wave mechanics for engineers and scientists*, vol. 2. world scientific publishing company, 1991.

[4] C. Swan and A. Callaghan, "Measurement data of ocean waves in the north sea," 2020.

[5] P. Schöpfer, "Non-linear irregular wave impact on monopile structures," Master's thesis, NTNU, 2016.

[6] F. Edition, J. Journée, and W. Massie, "Offshore hydromechanics," *Delft University of Technology*, 2001.

[7] M. Rahman, "Fundamentals concerning stokes waves," *WIT Transactions on Engineering Sciences*, vol. 9, 1970.

[8] D. Dermentzoglou, M. Castellino, P. De Girolamo, M. Partovi, G.-J. Schreppers, and A. Antonini, "Crownwall failure analysis through finite element method," *Journal of Marine Science and Engineering*, vol. 9, no. 1, p. 35, 2020.

[9] N. Mohd Zaki, M. Abu Husain, and G. Najafian, "Comparison of the extreme responses from different methods of simulating wave kinematics," in *MARINE VI: proceedings of the VI International Conference on Computational Methods in Marine Engineering*, pp. 365–376, CIMNE, 2015.

[10] T. B. Johannessen, "On the use of linear and weakly nonlinear wave theory in continuous ocean wave spectra: Convergence with respect to frequency," in *International Conference on Offshore Mechanics and Arctic Engineering*, vol. 48210, pp. 211–217, 2008.

[11] J. Wheeler, "Method for calculating forces produced by irregular waves," *Journal of petroleum technology*, vol. 22, no. 03, pp. 359–367, 1970.

[12] C. T. Stansberg, O. T. Gudmestad, and S. K. Haver, "Kinematics under extreme waves," *Journal of Offshore Mechanics and Arctic Engineering*, vol. 130(2), p. 021009, 2008.

[13] P. Schöpfer, "Non-linear irregular wave impact on monopile structures," Master's thesis, NTNU, 2016.

[14] M. Longuet-Higgins and R. Stewart, "Changes in the form of short gravity waves on long waves and tidal currents," *Journal of Fluid Mechanics*, vol. 8, no. 4, pp. 565–583, 1960.

[15] J. Zhang, "Nonlinear wave interaction and its applications to the analysis of steep ocean waves," in *Rogue Waves 2000: Proceedings of a Workshop Organized by Ifremer and Held in Brest, France, 29-30 November 2000, Within de Brest SeaTechWeek 2000*, vol. 32, p. 91, Editions Quae, 2001.

[16] D. N. Veritas, "Recommended practice dnv-rp-c205: environmental conditions and environmental loads," *DNV, Norway*, 2010.

[17] C. Spell, J. Zhang, and R. E. Randall, "Hybrid wave model for unidirectional irregular waves—part ii. comparison with laboratory measurements," *Applied Ocean Research*, vol. 18, no. 2-3, pp. 93–110, 1996.

[18] J. Zhang, L. Chen, M. Ye, and R. E. Randall, "Hybrid wave model for unidirectional irregular waves—part i. theory and numerical scheme," *Applied Ocean Research*, vol. 18, no. 2-3, pp. 77–92, 1996.

[19] J. Longridge, R. Randall, and J. Zhang, "Comparison of experimental irregular water wave elevation and kinematic data with new hybrid wave model predictions," *Ocean engineering*, vol. 23, no. 4, pp. 277–307, 1996.

[20] N. I. M. Zaki, M. K. A. Husain, G. Najafian, *et al.*, "Comparison of extreme surface elevation for linear and nonlinear random wave theory for offshore structures," in *MATEC Web of Conferences*, vol. 203, p. 01021, EDP Sciences, 2018.

[21] E. Bækkedal, "Alternative methods of realizing the sea spectrum for time-domain simulations of marine structures in irregular seas," Master's thesis, Institutt for marin teknikk, 2014.

[22] J. D. Fenton, "A fifth-order stokes theory for steady waves," *Journal of waterway, port, coastal, and ocean engineering*, vol. 111, no. 2, pp. 216–234, 1985.

A Interactions Between Two Waves

The following equations are the model for interactions between two waves developed by Longuet-Higgins & Stewart. The surface elevation is given by the following equation.

$$\eta = \eta_1 + \eta_2 + \frac{a_1 a_2}{2g}\{Ccos(\psi_1 - \psi_2) - Dcos(\psi_1 + \psi_2)\} \tag{20}$$

where

$$\psi_1 = (k_1 x - \omega_1 t)\ ;\ \psi_2 = (k_2 x - \omega_2 t) \quad [14]. \tag{21}$$

The velocity potential is given by the following equation.

$$\begin{aligned}\phi = \phi_1 + \phi_2 &+ \frac{E\cosh[(k_1 - k_2)(z+h)]\sin(\psi_1 - \psi_2)}{g(k_1 - k_2)\sinh(k_1 h - k_2 h) - (\omega_1 - \omega_2)^2\cosh(k_1 h - k_2 h)} \\ &+ \frac{F\cosh[(k_1 + k_2)(z+h)]\sin(\psi_1 + \psi_2)}{g(k_1 + k_2)\sinh(k_1 h + k_2 h) - (\omega_1 + \omega_2)^2\cosh(k_1 h + k_2 h)}\end{aligned} \tag{22}$$

where

$$\begin{aligned}C = &\frac{[2\omega_1\omega_2(\omega_1 - \omega_2)(1 + \alpha_1\alpha_2) + \omega_1^3(\alpha_1^2 - 1) - \omega_2^3(\alpha_2^2 - 1)](\omega_1 - \omega_2)(\alpha_1\alpha_2 - 1)}{\omega_1^2(\alpha_1^2 - 1) - 2\omega_1\omega_2(\alpha_1\alpha_2 - 1) + \omega_2^2(\alpha_2 - 1)} \\ &+ \omega_1^2 + \omega_2^2 - \omega_1\omega_2(\alpha_1\alpha_2 + 1)\end{aligned} \tag{23}$$

$$\begin{aligned}D = &\frac{([2\omega_1\omega_2(\omega_1 + \omega_2)(1 - \alpha_1\alpha_2) - \omega_1^3(\alpha_1^2 - 1) - \omega_2^3(\alpha_2^2 - 1)](\omega_1 + \omega_2)(1 + \alpha_1\alpha_2)}{\omega_1^2(\alpha_1^2 - 1) - 2\omega_1\omega_2(1 + \alpha_1\alpha_2) + \omega_2^2(\alpha_2 - 1)} \\ &+ \omega_1^2 + \omega_2^2 + \omega_1\omega_2(1 - \alpha_1\alpha_2)\end{aligned} \tag{24}$$

$$E = -\frac{1}{2}a_1 a_2[2\omega_1\omega_2(\omega_1 - \omega_2)(1 + \alpha_1\alpha_2) + \omega_1^3(\alpha_1^2 - 1) - \omega_2^3(\alpha_2^2 - 1)] \tag{25}$$

$$F = -\frac{1}{2}a_1 a_2[2\omega_1\omega_2(\omega_1 + \omega_2)(1 - \alpha_1\alpha_2) - \omega_1^3(\alpha_1^2 - 1) - \omega_2^2(\alpha_2^2 - 1)] \tag{26}$$

with

$$\alpha_1 = \frac{1}{\tanh(k_1 h)} \quad \text{and} \quad \alpha_2 = \frac{1}{\tanh(k_2 h)} \quad [14]. \tag{27}$$

B Equations for Surface Elevation and Velocity Potential Using 2^{nd} Order Random Wave Theory

The surface elevation calculated using 2^{nd} order random wave theory is given by Equation (28).

$$\eta = \frac{1}{4}\sum_{i=1}^{\infty}\sum_{j=1}^{\infty} a_i a_j \Bigg\{ \left[\frac{D_{ij}^{-} - (\mathbf{k}_i \cdot \mathbf{k}_j + R_i R_j)}{\sqrt{R_i R_j}} + (R_i + R_j)\right]\cos(\psi_i - \psi_j) + \left[\frac{D_{ij}^{+} - (\mathbf{k}_i \cdot \mathbf{k}_j - R_i R_j)}{\sqrt{R_i R_j}} + (R_i + R_j)\right]\cos(\psi_i + \psi_j)\Bigg\} \quad [21]. \tag{28}$$

The velocity potential is given by the following equation.

$$\phi = \frac{1}{4}\sum_{i=1}^{\infty}\sum_{j=1}^{\infty} b_i b_j \frac{\cosh k_{ij}^{-}(h+z)}{\cosh k_{ij}^{-} h}\frac{D_{ij}^{-}}{\omega_i - \omega_j}\sin(\psi_i - \psi_j) + \frac{1}{4}\sum_{i=1}^{\infty}\sum_{j=1}^{\infty} b_i b_j \frac{\cosh k_{ij}^{+}(h+z)}{\cosh k_{ij}^{+} h}\frac{D_{ij}^{+}}{\omega_i + \omega_j}\sin(\psi_i + \psi_j) \tag{29}$$

with

$$k_{ij}^{-} = |\mathbf{k}_i - \mathbf{k}_j| \quad \text{and} \quad k_{ij}^{+} = |\mathbf{k}_i + \mathbf{k}_j| \tag{30}$$

and

$$D_{ij}^{+} = \frac{(\sqrt{R_i} + \sqrt{R_j})\left[\sqrt{R_i}(k_j^2 - R_j^2) + \sqrt{R_j}(k_i^2 - R_i^2)\right]}{(\sqrt{R_i} + \sqrt{R_j})^2 - k_{ij}^{+}\tanh(k_{ij}^{+} h)} + \frac{2(\sqrt{R_i} + \sqrt{R_j})^2(\mathbf{k}_i \cdot \mathbf{k}_j - R_i R_j)}{(\sqrt{R_i} - \sqrt{R_j})^2 - k_{ij}^{+}\tanh(k_{ij}^{+} h)} \tag{31}$$

$$D_{ij}^{-} = \frac{(\sqrt{R_i} - \sqrt{R_j})\left[\sqrt{R_i}(k_i^2 - R_i^2) + \sqrt{R_i}(k_j^2 - R_j^2)\right]}{(\sqrt{R_i} + \sqrt{R_j})^2 - k_{ij}^{-}\tanh(k_{ij}^{-} h)} + \frac{2(\sqrt{R_i} - \sqrt{R_j})^2(\mathbf{k}_i \cdot \mathbf{k}_j + R_i R_j)}{(\sqrt{R_i} - \sqrt{R_j})^2 - k_{ij}^{-}\tanh(k_{ij}^{-} h)} \tag{32}$$

with

$$R_i = k_i \tanh(k_i h) \quad [21]. \tag{33}$$

C Measured Surface Elevation

Figure 6 shows the surface elevation for the measurement data [4].

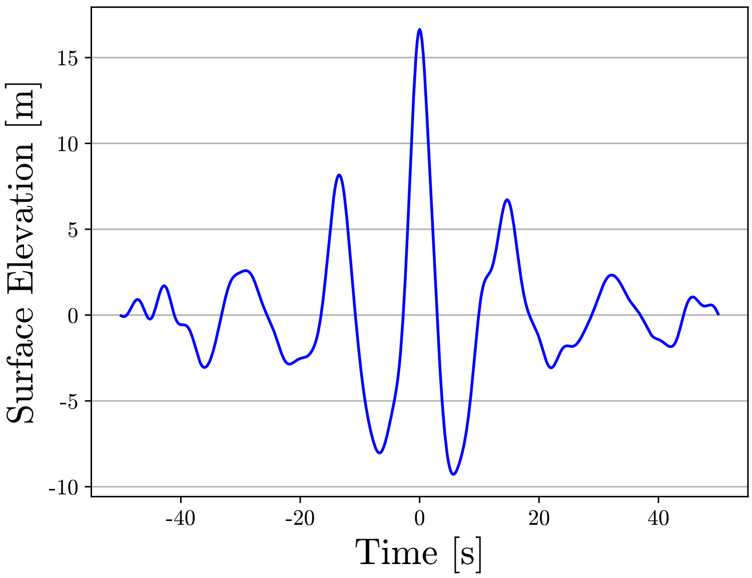

Figure 6: The measured water surface elevation [4].

D Measured Amplitude Spectrum

Figure 7 shows the frequency spectrum for measured amplitude [4].

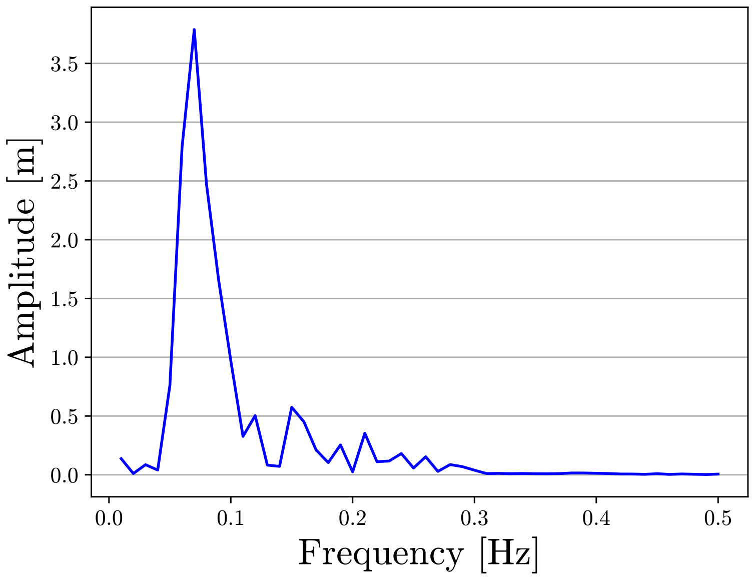

Figure 7: The frequency spectrum for measured amplitude [4].

E Equations for Stokes' 5$^{\text{th}}$ Order Theory

The following equations is Stokes' 5$^{\text{th}}$ order solution for surface elevation and velocity potential.

$$k\eta(x) = kh + \epsilon\cos(kx) + \epsilon^2 B_{22}\cos(2kx) + \epsilon^3 B_{31}[\cos(kx) - \cos(3kx)] + \epsilon^4[B_{42}\cos(2kx) + B_{44}\cos(4kx)] + \epsilon^5[-(B_{53}+B_{55})\cos(kx) + B_{53}\cos(3kx) + B_{55}\cos(5kx)] \tag{34}$$

$$\phi(x,z) = -cx + c_o\left(\frac{g}{k^3}\right)^{\frac{1}{2}}\sum_{i=1}^{5}\epsilon^i\sum_{j=1}^{i}A_{ij}\cosh(jkz)\sin(jkx) \tag{35}$$

where $\epsilon = Hk/2$ and

$$B_{22} = \coth(kh)\left(\frac{1+2S}{2(1-S)}\right) \tag{36}$$

$$B_{31} = \frac{-3(1+3S+3S^2+2S^3)}{8(1-S)^3} \tag{37}$$

$$B_{42} = \coth(kh)\frac{6-26S-182S^2-204S^3-25S^5+26S^5}{6(3+2S)(1-S)^4} \tag{38}$$

$$B_{44} = \coth(kh)\frac{24+92S+122S^2+66S^3+67S^4+34S^5}{24(3+2S)(1-S)^4} \tag{39}$$

$$B_{53} = 9\frac{132+17S-2.216S^2-5.897S^3-6.292S^4-2.687S^5+194S^6+467S^7+82S^8}{128(3+2S)(4+S)(1-S)^6} \tag{40}$$

$$B_{55} = 5\frac{300+1.579S+3.176S^2+2.949S^3+1.188S^4+675S^5+1.326S^6+827S^7+130S^8}{384(3+2S)(4+S)(1-S)^6} \tag{41}$$

where $S = \text{sech}(2kh)$ [22].